

Angular distribution of a pulse of low-energy phonons in liquid ^4He

Ruslan V. Vovk, Charles D. H. Williams, and Adrian F. G. Wyatt
 School of Physics, University of Exeter, Exeter EX4 4QL, United Kingdom
 (Received 2 April 2003; published 6 October 2003)

We have made time-resolved measurements of the angular distribution of low-energy phonons (l -phonons) that are created by a heater in liquid helium, at several powers and pulse lengths, in order to investigate the temporal and spatial development of such l -phonon pulses. The angular distributions show a mesa shape with a flat top in the direction normal to the heater. The width of the flat top increases with power and pulse length. We argue that the flat top is due to the creation of high-energy phonons (h -phonons). These are created until the temperature of the central region of the l -phonon sheet reaches 0.7 K, when the creation of h -phonons essentially stops. Outside the flat top, the angular distribution is due to the lateral spreading of the l -phonon sheet. A model for this is described in the preceding paper [I.N. Adamenko, K. E. Nemchenko, V.A. Slipko, and A.F.G. Wyatt, preceding paper, Phys. Rev. B **68**, 134507 (2003)] which gives a framework for considering these measurements.

DOI: 10.1103/PhysRevB.68.134508

PACS number(s): 67.40.Fd

I. INTRODUCTION

It has become apparent, in the past few years, that a propagating pulse of phonons injected into liquid ^4He is an extremely anisotropic phonon system.¹⁻⁵ This is because the phonon-phonon interactions are extremely angular dependent.^{6,7} The interaction between low-energy phonons (l -phonons) is predominantly through the three-phonon process (3pp),⁸⁻¹⁰ which involves angles between phonons of $\approx 8^\circ$ for phonons at a temperature ~ 1 K.⁵ This means that if phonons are created in a narrow range of angles then the interactions between them do not tend to broaden the angular range very quickly. Indeed, a measurement of the angular width of those low-energy phonons, after a distance of 15.6 mm, has found a distribution with half-width at half-maximum (hwhm) = 10.5° .² Besides the rapid 3pp scattering there is a much slower 4pp interaction.¹¹⁻¹³ The primary effect of this is to scatter l -phonons to energies $E_p > 10$ K where they are relatively very stable. These high energy phonons (h -phonons) cannot spontaneously decay, in contrast to the ones with $E_p < 10$ K. So if the liquid helium temperature is low enough, the h -phonons can propagate in a ballistic pulse through the helium. These phonons have been detected,^{14,1-3} and their production analyzed.^{4,5} One of the striking characteristics of the h -phonon pulse is that it has an even narrower cone angle than the l -phonons. The hwhm can be as small as 3.5° .²

It is interesting to consider how a l -phonon pulse develops spatially as it propagates. The injected pulse dimensions are governed by the heater (1×1 mm²) and the pulse length (typically $t_p = 50$ ns) so the l -phonons are in thin sheet, ct_p thick, typically 10^{-2} mm. After 17 mm, an angular half-width of 10.5° is equivalent to a lateral half-width of 3.1 mm. The possibility that the l -phonons simply expand geometrically at the measured cone angle has been analyzed.¹⁵ It turns out that this expansion leads to rapid cooling of the l -phonons. This happens because the energy density of the l -phonons is proportional to the area of the phonon sheet, as there is essentially no time dispersion in the direction of propagation, and the pulse temperature T is proportional to

$E^{1/4}$. As the production rate of h -phonons strongly decreases with decreasing temperature, geometric expansion results in the h -phonons only being created near the heater. This is contrary to observation³ which means that the l -phonon expansion is not geometric.

In order to investigate this l -phonon propagation further we have made new measurements of the angular distribution of l -phonons at several powers and pulse lengths. In parallel, a theoretical model of the l -phonon pulse has been developed.¹⁶ We describe the experiment in Sec. II, present the results in Sec. II, and discuss them in Sec. IV. In Sec. V, we give our conclusions.

II. THE EXPERIMENT

The experiment in essence is simply a thin-film heater H_1 that can rotate about an axis that lies in its plane and through its center. A distance from it, in this case 16.7 mm, is a bolometer B_4 which detects the phonon pulses. This is shown schematically in Fig. 1. We actually had three bolometers positioned so we could check that the normal to the

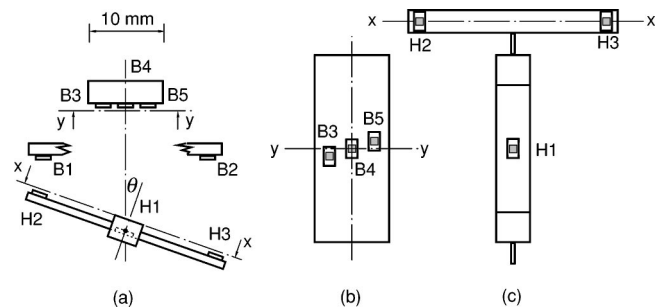


FIG. 1. Schematic drawings of the experimental arrangement. The heater H_1 is rotated by a stepping motor through a set of pulley wheels, not shown. The center bolometer B_4 is used for all the data in the figures except Fig. 2. The separation of the heater H_1 and the center bolometer B_4 is 16.7 mm. The heaters H_2 and H_3 on the arms and the fixed bolometers B_1 and B_2 are used to measure the rotation angle θ .

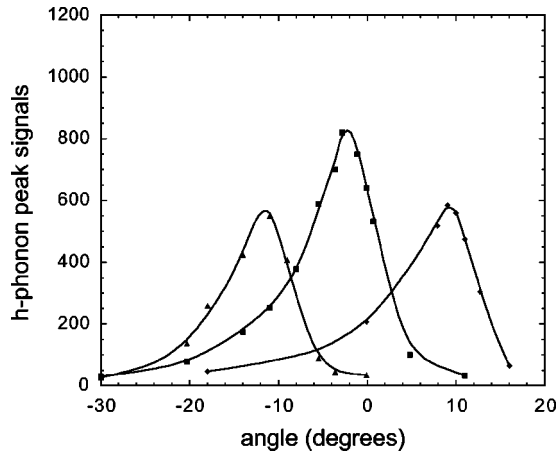


FIG. 2. The peaks of the high-energy phonon signals, from the three bolometers B_3 , B_4 , and B_5 vs heater angle are shown. The symmetrical distribution of the three plots shows that the normal to the heater sweeps through the center bolometer B_4 .

heater swept in an arc that passes through the central bolometer B_4 . This is an important detail as otherwise some structure of the pulse, along the normal direction, could be missed.

The heater is rotated by a stepping motor through a set of pulley drives to gear down the angular step size. The motor has a step size of 18° and the corresponding heater platform step is 1° . The angle of the heater is measured with separate heaters on extended arms which send phonon pulses to fixed bolometers. The distance between these heaters and bolometers is found by time of flight and so the rotation angle can be calculated. The angular resolution is 0.2° with a possible systematic uncertainty of about 2° . However, we can use the h -phonon distribution, which is much more sharply peaked than the l -phonons (compare Figs. 2 and 3), to determine the zero-angle position.

The bolometers are superconducting zinc films, scratched into a serpentine track covering 1 mm^2 . The zinc transition temperature is lowered with a steady magnetic field applied

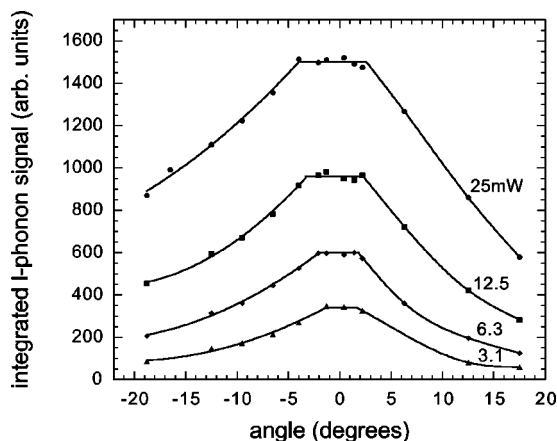


FIG. 3. The low-energy phonon signal, integrated over time, vs heater angle for a range of heater powers is shown. The flat top of the distributions is clearly apparent and increases with power. The pulse length is 50 ns and the lines are guides for the eye.

perpendicular to the plane of the films. The bolometer was held at a constant temperature by a fast electronic circuit.^{17–19} The cell is filled with isotopically pure ^4He (Ref. 20) and is cooled by a helium dilution refrigerator. The data are taken at temperatures $< 60 \text{ mK}$ where it is temperature independent. The data are recorded with a Tektronix DSA601A signal averager.

III. RESULTS

To check the alignment of the heater normal and the center bolometer, the peak of the h -phonon signals from the three bolometers was measured as a function of angle, see Fig. 2. The angular separation of the peaks corresponds to the offset positions of the bolometers. We see that the central bolometer gave a larger signal than the other two. This size difference is due to the bolometers being offset by $\pm 3^\circ$ in the direction perpendicular to the rotation plane. The disposition and size of the peaks in Fig. 2 indicate that the central bolometer lies in the rotation plane of the heater normal.

The phonon pulses are measured at various heater powers and pulse lengths. The detected signals show both the l - and h -phonons, however, in this paper we mainly restrict our discussion to the l -phonons so we can consider them in the light of the preceding paper.¹⁶ In Fig. 3 we show time-integrated l -phonon signals from the central bolometer B_4 for a heater pulse length of 50 ns as a function of angle for several powers. The significant feature of this data is the clear mesa shape of the angular distribution. We see that the angular width of the flat top increases with pulse power, but slower than linearly. Due to the finite size of the bolometer, whose full width subtends an angle 3.4° at the heater, the actual full widths of the flat tops are broader than the measured ones, by this amount. With this correction, the area of the flat top increases approximately as the square root of the heater power.

We believe that the mesa shape is due to the creation of h -phonons in the hot central region of the l -phonon sheet. The creation of h -phonons takes energy from the l -phonons in this region and so reduces their contribution to the signal. The creation of h -phonons continues to extract energy until the l -phonon temperature drops to $\approx 0.7 \text{ K}$ where the creation rate is very low. So we see that the flat top is due to the central region of the sheet having the same temperature of $\approx 0.7 \text{ K}$, and is a result of the initial hot central region of the l -phonon sheet, which is predicted in the preceding paper.¹⁶ However, it is not the same flat top shown there as the calculated shape ignores h -phonon creation. If the flat top of the mesa is at 0.7 K then the sides of the mesa must be at temperature $< 0.7 \text{ K}$ because the bolometer responds to the energy density in the sheet. This lower temperature is due to the in-plane expansion of the l -phonon sheet. These outer regions have never been as hot as the central region of the sheet, and they have produced a smaller number of h -phonons and at distances nearer to the heater.

The picture, outlined above, suggests that the sum of the energies in the l - and h -phonons would not have the mesa-shaped angular dependence, but would show a simple rounded peak without any truncation. However we do not

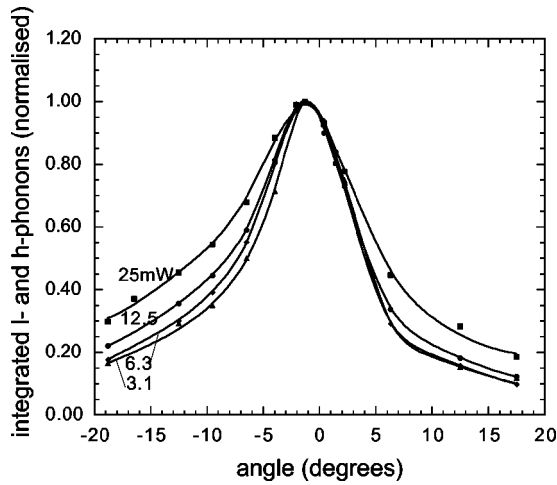


FIG. 4. The sum of the low- and high-energy phonon signals, scaled to account for the bolometer responsivities (see text) and integrated over time, are shown against heater angle for several powers. The pulse length is 50 ns and the lines are guides for the eye. Compared with Fig. 3, these curves have a narrow and rounded peak which is consistent with the truncation of the low-energy phonon angular distribution being due to the loss of high-energy phonons.

expect this total energy to exactly reproduce the *l*-phonon behavior, when no *h*-phonons are created, for two reasons. First, removing energy from the *l*-phonon sheet affects the subsequent lateral expansion. Second, the *h*-phonons once created are only weakly interacting and so only expand due to their ballistic propagation directions which have a small angular range.

The sum of *l*- and *h*-phonon energies cannot be found by simply integrating the measured signal over time because the responsivity of the bolometer depends on the energy of the phonons. The modal energy of the *l*-phonons is $\epsilon_l \sim 2k_B T$ where *T* is their temperature. By the time the *l*-phonons reach the bolometer, their temperature has dropped to $T \approx 0.7$ K, so $\epsilon_l \approx 1.4$ K. The *h*-phonons have energy $\epsilon_h \geq 10$ K. Now the sensitivity of the bolometer depends on the probability that a phonon in the helium can transmit into the solid zinc. This has been found to be proportional to the energy of the phonon up to an energy of 5 K and constant thereafter.²¹ So the ratio of the responsivities to *l*- and *h*-phonons is 1.4–5.

We have integrated the *l*- and *h*-phonon signals separately and multiplied the *h*-phonon integral by $1.4/5 = 0.28$ before adding them to the *l*-phonon integral. The result is shown in Fig. 4 as a function of angle. We see that the peak is now rounded and narrow. For heater pulses of 6.3 mW and 50 ns the *h*-phonons are contributing, at the peak, about 2.5 times that of the *l*-phonons, but at 11° from the peak, the contributions are about equal. This is because the *h*-phonons are confined to narrower cone angles than the *l*-phonons.

We also see in Fig. 4 that, as the power is reduced, the angular dependence tends to a limiting shape. At high powers, when the *h*-phonon density is high, we expect the *h*-phonons to interact and scatter into low-energy phonons by the 4pp process $h_1 + h_2 = h_3 + l_4$. The low-energy phonons created in this process will rapidly decay by 3pp. They will

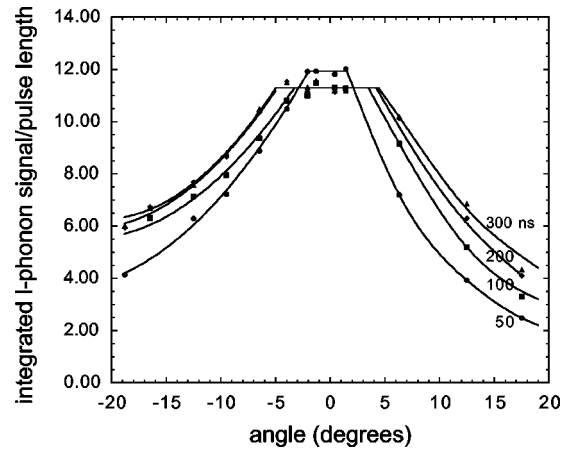


FIG. 5. The low-energy phonon signal, integrated over time and divided by the pulse length, vs heater angle for several pulse lengths is shown. The heater power is 6.3 mW. The lines are guides for the eye. It can be seen that the flat top increases with pulse length but saturates at long pulse lengths.

arrive within the *h*-phonon pulse and, in general, will have a broader angular distribution. Their contribution is under represented because of the reduced responsivity of the bolometer to these low-energy phonons. The measured energy will therefore appear smaller at small angles where the *h*-phonons are created. This will cause the angular distribution to appear wider at higher powers as the signal is depressed in the central regions.

In Fig. 5 we show the angular dependence at different pulse lengths for a constant heater power of 6.25 mW. We plot the integrated *l*-phonon signal divided by the pulse length. At $\theta = 0$, this quantity is nearly independent of pulse length up to $t_p = 300$ ns, see Fig. 6. Nevertheless the plateau in Fig. 5, for 50-ns data, is slightly higher than for other pulse lengths. We would expect the integrated signal to be proportional to pulse length if the region at the center of the *l*-phonon pulse cools to the same temperature of 0.7 K irrespective of the pulse length, as then the signal is just propor-

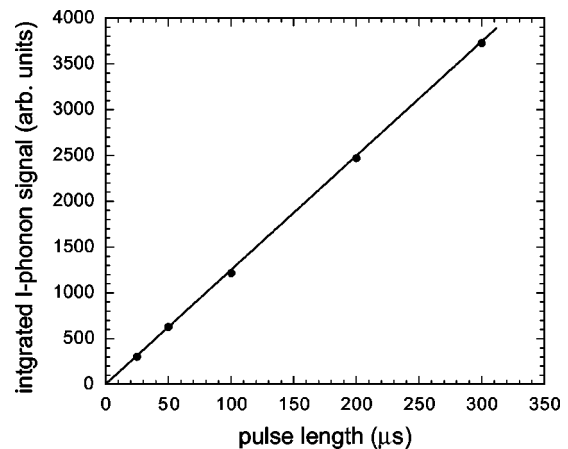


FIG. 6. The low-energy phonon signal at the angular peak, integrated over time, is shown as a function of pulse length. The heater power is 6.3 mW. Slightly higher signal for 50 ns in Fig. 5 is not visible on this scale.

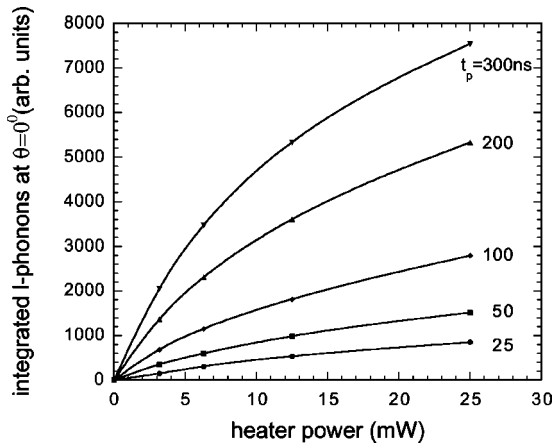


FIG. 7. The low-energy phonon signal, integrated over time, is shown as a function of power at different pulse lengths. It can be seen that the low-energy phonons increase relatively more slowly with power at longer pulse lengths. The lines are guides for the eye.

tional to the thickness of the l -phonon sheet. The mesa shape is again apparent and the width of the flat top increases with pulse length, but saturates at ≈ 300 ns. This indicates that pulse cools as a whole and the increased pulse thickness means that there is more energy at larger angles to create h -phonons before it cools to the temperature of ≈ 0.7 K, where no more h -phonons are created. The saturation of the width of the flat top, with pulse length, is probably due to the pulse becoming so long that h -phonons stay mainly within the l -phonon pulse.

In Fig. 7 we show the integrated l -phonon signal as a function of power at different pulse lengths at $\theta=0$. We see that at low power the energy in the l -phonons increases linearly with pulse length. Also, this energy increases with heater power but more slowly at higher powers and longer pulse lengths. We believe this is mainly due to an increase in the occupied solid-angle in momentum space. At higher powers, a larger fraction of the l -phonon energy is lost to the creation of h -phonons than at lower powers.

IV. DISCUSSION

The angular distributions of the l -phonons show a unique and remarkable shape. They have a flat top over a range of angles about zero and outside this region the l -phonon signal falls smoothly. The overall shape is reminiscent of a mesa. As the bolometer is responsive to the energy density in the sheet of l -phonons, this shows that the energy density, and hence the temperature of the sheet, is constant over the central region. We attribute this singular behavior to the creation of h -phonons.

The h -phonons are most rapidly created in the hottest region of the l -phonon sheet; the creation varies as $\sim \exp(-\epsilon/T)$ where $\epsilon=3$ K and T is the local temperature of the l -phonon sheet.⁷ As they are created, the temperature of the l -phonon sheet drops until it reaches ~ 0.7 K when the creation of h -phonons essentially stops. This produces a central region of the l -phonon sheet at a uniform temperature of ~ 0.7 K, at relatively large distances from the heater. After

the temperature has reached ~ 0.7 K it will then fall more slowly due to the in-plane expansion of the l -phonon sheet. The region of the sheet, outside this central area, is cooler than the central area at all distances and it cools mainly through in-plane expansion. This is because at the lower temperature, the h -phonon production is much reduced. As the power in the pulse increases, the l -phonon pulse is hotter over a wider angular range and so h -phonons are created over a wider angular range. This makes the flat top, in the measured angular distribution, wider.

It is apparent in Figs. 2, 3, 4, and 5 that there is an asymmetry in the data about $\theta=0^\circ$. This must be due to the heater as nothing else can break the symmetry. The temperature of the 1 mm^2 gold film heater is determined by the resistivity, which may be a function of position, and its geometrical shape. It appears from the asymmetry that the current density, and hence the temperature, is not uniform. The asymmetry of the phonon distribution is a clear indication that the l -phonons in the sheet are strongly interacting when their momenta are in a cone of angle θ_{3pp} at each point, but between points in the plane of the sheet, the coupling is relatively weak. This means that the temperature of the l -phonons can vary across the sheet at all sensible propagation distances.

If we consider a contrary scenario—that the l -phonons are not interacting and so travel ballistically from the heater to the bolometer, then a temperature variation over a distance, say, 0.5 mm at the heater would give overlapping phonon angular distributions at the bolometer, separated by the same lateral distance 0.5 mm. This would give a negligible asymmetry in the combined angular distributions. So the detected asymmetry, although unintentional, is actually good evidence for the strongly interacting model in the preceding paper.¹⁶

We are unable at present to measure the angular distribution of l -phonon pulses at such a low temperature (<0.7 K) that essentially no h -phonons are created. The signals just disappear into the noise, especially at larger angles where the signals are smaller. This means that our results are not directly comparable with the model.¹⁶ However, our results are consistent with a laterally developing l -phonon pulse as described by the model, together with the production of h -phonons. The model of a l -phonon sheet with a hot central region is one reason why the h -phonons are detected over a narrower angle than the l -phonons as h -phonon creation is faster at higher temperatures. Also the model result—that the hot central region persists for large distances from the heater, albeit with some cooling after ~ 5 mm—explains why h -phonons are created over most of the l -phonon propagation path.

Further development of the model and measurement of the angular distribution at different distances are required for a detailed comparison between the two.

V. CONCLUSIONS

We have presented measurements of the angular distribution of l -phonons that are created by a heater, at several powers and pulse lengths. The angular distributions are remarkable; they show a mesa shape, and the width of the flat

top increases with power and pulse length. The flat top of the distribution is due to the creation of high-energy phonons which leaves the central region of the l -phonon sheet at the same temperature ~ 0.7 K. At the lowest power and shortest pulse length the creation of h -phonons is relatively small but not negligible. Under these conditions, the flat top is just resolvable. The width of the flat top saturates at a pulse length ~ 300 ns where it is in the long pulse regime. However, the width of the flat top goes on increasing with power in the range that we have explored.

We have shown that the total energy of the l - and h -phonons does not have a mesa-shaped distribution but has a narrow and rounded peak. This confirms that the missing energy in the l -phonon sheet has been converted into h -phonons. We noted that the angular distribution of the

l -phonons will develop differently if energy is lost from it to h -phonons, so the angular distribution of the sum of the l - and h -phonon energies cannot be directly compared to the model in the preceding paper.¹⁶ Nonetheless the measurements are consistent with this model which gives a framework for analyzing the temporal and spatial development of phonon pulses in liquid helium.

ACKNOWLEDGMENTS

We would like to thank I. N. Adamenko for many useful discussions and D.H.S. Smith for help with collecting the data, EPSRC for Grants Nos. GR/N20225 and GR/N18796, and S. Tuckett for constructing the rotating apparatus.

-
- ¹M.A.H. Tucker and A.F.G. Wyatt, *J. Phys.: Condens. Matter* **6**, 2813 (1994).
- ²M.A.H. Tucker and A.F.G. Wyatt, *J. Phys.: Condens. Matter* **6**, 2825 (1994).
- ³M.A.H. Tucker and A.F.G. Wyatt, *J. Low Temp. Phys.* **113**, 621 (1998).
- ⁴I.N. Adamenko, K.E. Nemchenko, A.V. Zhukov, M.A.H. Tucker, and A.F.G. Wyatt, *Phys. Rev. Lett.* **82**, 1482 (1999).
- ⁵A.F.G. Wyatt, M.A.H. Tucker, I.N. Adamenko, K.E. Nemchenko, and A.V. Zhukov, *Phys. Rev. B* **62**, 9402 (2000).
- ⁶I.N. Adamenko, K.E. Nemchenko, and A.F.G. Wyatt, *J. Low Temp. Phys.* **125**, 1 (2001).
- ⁷I.N. Adamenko, K.E. Nemchenko, and A.F.G. Wyatt, *J. Low Temp. Phys.* **126**, 1471 (2002).
- ⁸H.J. Maris and W.E. Massey, *Phys. Rev. Lett.* **25**, 220 (1970).
- ⁹S. Havlin and M. Luban, *Phys. Lett. A* **42**, 133 (1972).
- ¹⁰M.A.H. Tucker, A.F.G. Wyatt, I.N. Adamenko, A.V. Zhukov, and K.E. Nemchenko, *Low Temp. Phys.* **25**, 488 (1999).
- ¹¹I.M. Khalatnikov, *An Introduction to the Theory of Superfluidity* (Addison Wesley, Redwood City, California, 1989).
- ¹²S.G. Eckstein, Y. Eckstein, J.B. Ketterson, and J.H. Vignos, *Physical Acoustics* (Academic Press, New York, 1970), Vol. II, p. 244.
- ¹³M.A.H. Tucker and A.F.G. Wyatt, *J. Phys.: Condens. Matter* **4**, 7745 (1992).
- ¹⁴M. Brown and A.F.G. Wyatt, *Physica B* **195–196**, 495 (1990).
- ¹⁵A.F.G. Wyatt, I.N. Adamenko, and K.E. Nemchenko, *J. Low Temp. Phys.* **126**, 609 (2002).
- ¹⁶I.N. Adamenko, K.E. Nemchenko, V.A. Slipko, and A.F.G. Wyatt, preceding paper, *Phys. Rev. B* **68**, 134507 (2003).
- ¹⁷R.A. Sherlock and A.F.G. Wyatt, *J. Phys. E* **16**, 673 (1983).
- ¹⁸R.A. Sherlock, *J. Phys. E* **17**, 386 (1984).
- ¹⁹C.D.H. Williams, *Meas. Sci. Technol.* **1**, 322 (1990).
- ²⁰P.C. Hendry and P.V.E. McClintock, *Cryogenics* **27**, 131 (1987).
- ²¹T.W. Bradshaw and A.F.G. Wyatt, *J. Phys. C* **16**, 651 (1983).